Hindawi
Journal of Function Spaces
Volume 2022, Article ID 9637098, 9 pages
https://doi.org/10.1155/2022/9637098

Research Article

Fractional Complex Transform and Homotopy Perturbation Method for the Approximate Solution of Keller-Segel Model

Xiankang Luo,[1] **Muhammad Nadeem**,[1] **Mustafa Inc**,[2,3,4] **and Suliman Dawood**[5]

[1]Faculty of Science, Yibin University, 644000 Yibin, China
[2]Department of Computer Engineering, Biruni University, Istanbul, Turkey
[3]Science Faculty, Department of Mathematics, Firat University, 23119 Elazig, Turkey
[4]Department of Medical Research, China Medical University, Taichung, Taiwan
[5]Department of Mathematics, Sheba Region University, Marib, Yemen

Correspondence should be addressed to Muhammad Nadeem; nadeem@yibinu.edu.cn
and Suliman Dawood; sulimanseddek@usr.ac

Received 17 June 2022; Revised 28 June 2022; Accepted 14 July 2022; Published 28 July 2022

Academic Editor: Yusuf Gurefe

In this paper, we propose an innovative approach to determine the approximate solution of the coupled time-fractional Keller-Segel (K-S) model. We use the fractional complex transform (FCT) to switch the model into its differential partner, and then, the homotopy perturbation method (HPM) is introduced to tackle its nonlinear elements using He's polynomials. This two-scale theory helps to define the physical meaning of the FCT for the solution of the K-S model. Some examples are illustrated to show that the proposed scheme presents the significant results. The considerable findings show that this strategy does not require any assumptions and also reduces the massive computations without imposing any constraints. This technique is also suitable in functional studies of fractal calculus due to its powerful and robust support for nonlinear problems.

1. Introduction

Fractional differential equations (FDEs) are the generalizations of classical differential equations with integer orders. It is worth reporting that some mathematical models of integer-order derivatives particularly nonlinear models do not work adequately for most of the cases [1–3]. This is because integer order derivatives are limited operators and are inappropriate for infinite variance whereas fractional order derivatives are worldwide to take account of the domination of the neighborhood. In recent years, nonlinear FDEs in mathematical physics are competing against a principal role in miscellaneous domains, such as biological science, applied science, signal processing, control theory, finance, and fractal dynamics [4–7].

In 1970, Keller and Segel introduced a hypothesis to express the combination system of cellular slime mold by chemical fascination. The K-S model has broadly been practiced for chemotaxis terms due to its competency to capture the key facts and its impulsive nature. The significance of chemotaxis has achieved much attraction due to its crucial function in a broad variety of biological occurrences [8, 9]. In this article, we examine the coupled time-fractional K-S model of the form

$$\begin{aligned} \frac{\partial^\delta \eta}{\partial \wp^\delta} &= a\frac{\partial^2 \eta}{\partial \mathfrak{I}^2} - \frac{\partial}{\partial \mathfrak{I}}\left(\eta \frac{\partial}{\partial \mathfrak{I}}\chi(\varsigma)\right), \\ \frac{\partial^\delta \varsigma}{\partial \wp^\delta} &= b\frac{\partial^2 \varsigma}{\partial \mathfrak{I}^2} + cu - dv, \end{aligned} \tag{1}$$

subject to the initial solutions, we get

$$\begin{aligned} \eta(\mathfrak{I},0) &= \eta_0(\mathfrak{I}), \\ \varsigma(\mathfrak{I},0) &= \varsigma_0(\mathfrak{I}), \end{aligned} \tag{2}$$

where $\eta(\Im, \wp)$ and $\varsigma(\Im, \wp)$ represent the bacterial density and the concentration of chemical substance as a function of $\Im$ and $\wp$, respectively, and $D_{\Im}(\eta(\Im,\wp)D_{\Im}\chi(\varsigma))$ denotes the chemotactic term and shows that the cells are sensitive to the chemicals and are attracted by them [10]. The sensitivity function $\chi(\varsigma)$ is a smooth function which describes the cell's perception and response to the chemical stimulus ς while $a, b, c,$ and d are positive constants. If $\delta = 1$, the time-fractional K-S model (1) leads to a simple nonlinear differential equation that has been studied extensively whereas $D_{\wp}^{\delta}$ taken as Caputo's sense [11] and $D_{\wp}^{\delta} = \partial^{\delta}/\partial\wp^{\delta}$ is He's fractional derivative defined [12, 13]

$$\frac{\partial^{\delta}\eta}{\partial\wp^{\delta}} = \frac{1}{\Gamma(n-\delta)}\frac{d^n}{dt^n}\int (s-\wp)^{n-\delta-1}[\eta_0(s) - \eta(s)]ds. \quad (3)$$

Many actions in physics and engineering can be precisely characterized by utilizing differential equations with various sorts of fractional derivatives. The finding of the approximate and exact solution of FDEs is a very crucial challenge. There have been a lot of developments to solve FDEs in nonlinear dynamics. FDEs are used extensively because they do not have exact solutions, and thus, approximate and numerical solutions are needed. The homotopy perturbation method (HPM) [14] is one of the most famous approaches to achieve the series solutions of linear and nonlinear differential equations of arbitrary orders. Later, various methods have been developed to show that HPM a is very efficient and powerful tool for finding the approximate solution to FDEs [15–18]. In order to get the solution of the K-S model, many powerful and efficient techniques have been suggested to obtain the analytical solutions such as Laplace homotopy perturbation method [19], iterative method [20], homotopy perturbation Sumudu transform [21], and natural homotopy transform method [22] with a logic sensitivity function and small diffusivity. Some partial differential equations with fractional order are not easy to solve, and then, their approximate solution can be evaluated. The two-scale approach converts the fractional order to a simple partial differential equation which is now easy to solve by the homotopy perturbation method.

This study presents the idea of a two-scale method to obtain the solution of the fractional K-S model in Caputo sense. The FCT converts the model into its differential partner, and then, HPM is introduced to bring down the nonlinear terms in algebraic series. The quality of the current method is appropriate to provide the analytical results to the given examples. This study is summarized as follows: In Section (2), we recall some basic definitions of fractional calculus. We present the idea of the homotopy perturbation method and the two-scale approach in Sections (3) and (4), respectively. Some numerical examples are provided to demonstrate the performance of this approach in Section (5) and the discussion of results in Section (6). The conclusion is given in Section (7).

2. Preliminary Concepts

Definition 1. The Riemann-Liouville fractional integral operator of order $\delta > 0$ of a function $f(t) \in C_{\mu}$, $\mu \geq -1$, is defined as [23]

$$J^{\delta} f(\wp) = \frac{1}{\Gamma(1+\delta)}\int_0^{\wp}(\wp-\tau)f(\tau)d\tau, \quad J^0 f(\wp) = f(\wp). \quad (4)$$

Definition 2. The Caputo fractional derivative of $f(\wp)$ in the Caputo sense is given [23]

$$D^{\gamma}w(\Im,\wp) = \begin{cases} \dfrac{1}{\Gamma(\gamma-\delta)}\displaystyle\int_0^{\wp}(\wp-\tau)^{\gamma-\delta-1}\frac{\partial^{\gamma}w(\Im,\wp)}{\partial\tau^{\gamma}}d\tau, & \gamma-1<\delta<\gamma, \\ \dfrac{\partial w(\Im,\wp)}{\partial\wp^{\gamma}}, & \delta=\gamma\in\mathbb{N}. \end{cases} \quad (5)$$

Lemma 3. *If $\gamma - 1 < \delta \leq \gamma$, $\gamma \in \mathbb{N}$, $\wp>0$, $w \in C_{-1}^{\gamma}$, then*

$$D^{\delta}J^{\delta}w(\wp) = w(\wp),$$
$$D^{\delta}J^{\delta}w(\wp) = w(\wp) - \sum_{k=0}^{\gamma-1} w^k(0^+)\frac{\wp^k}{k!}, \quad \wp > 0. \quad (6)$$

The fractional derivatives are considered in Caputo sense which allows the conditions to deal with the expression of the problems.

3. Basic Idea of the Homotopy Perturbation Method

In this segment, we explain the fundamental concept of HPM. Let the following nonlinear equation [24]

$$L(\eta) - f(\varrho) = 0, \varrho \in \Upsilon, \quad (7)$$

with boundary conditions

$$B\left(\eta, \frac{\partial\eta}{\partial n}\right) = 0, \quad \varrho \in \Theta, \quad (8)$$

where L is a general function with boundary operator $B, f(\varrho)$ is analytic function, and Θ is the boundary of the domain Υ. The operator L can normally be separated into two operators with M as a linear and N being a nonlinear operator. Thus, Equation (7) can be accompanied as follows:

$$M(\eta) + N(\eta) - f(\varrho) = 0. \quad (9)$$

Let us consider $\varsigma(r, p): \Upsilon \times [0, 1] \longrightarrow \mathbb{R}$ that confirms or

$$H(\varsigma, q) = (1-q)[L(\varsigma) - M(\eta_0)] + q[L(\varsigma) - N(\varsigma) - f(\varrho)], \quad (10)$$

$$H(\varsigma, q) = L(\varsigma) - M(\eta_0) + qM(\eta_0) + q[N(\varsigma) - f(\varrho)] = 0, \tag{11}$$

where $q \in [0, 1]$ is said to be a homotopy parameter and η_0 is an initial approximation of Equation (7). According to HPM, we can take q as a small element, and suppose that the solution of Equation (11) can be written as a power series of q:

$$\varsigma = \varsigma_0 + qv_1 + q^2\varsigma_2 + \cdots. \tag{12}$$

Considering $q = 1$, the approximate solution of Equation (7) is obtained as follows:

$$\eta = \lim_{q \longrightarrow 1} \varsigma = \varsigma_0 + \varsigma_1 + \varsigma_2 + \varsigma_3 + \cdots. \tag{13}$$

Using Equations (11) and (12), we can identify the similar powers of q to obtain the following series solution form:

$$\begin{aligned} q^0 &: \varsigma_0 - f(\mathfrak{I}) = 0, \\ q^1 &: \varsigma_1 - H(\varsigma_0) = 0, \\ q^2 &: \varsigma_2 - H(\varsigma_0, \varsigma_1) = 0, \\ q^3 &: \varsigma_3 - H(\varsigma_0, \varsigma_1, \varsigma_2) = 0, \\ &\vdots, \end{aligned} \tag{14}$$

where $H(\varsigma_0, \varsigma_1, \varsigma_2, \cdots, \varsigma_j)$ depending upon $\varsigma_0, \varsigma_1, \varsigma_2, \cdots, \varsigma_j$ called He's polynomials can be computed by adopting the following rule:

$$H(\varsigma_0, \varsigma_1, \varsigma_2, \cdots, \varsigma_j) = \frac{1}{j!} \frac{\partial^j}{\partial q^j} N\left(\sum_{i=0}^{j} \varsigma_i q^i\right)\Bigg|_{q=0}. \tag{15}$$

The system of nonlinear equations in (14) is evidently simple to calculate, and thus, the components $\varsigma_i, i \geq 0$ of HPM can be identified easily which leads to the series solutions very rapidly.

4. Fractional Complex Transform

The dimension and scale are highly important elements due to its impressive outcomes and properties of the configuration through the modeling of a problem. FCT is a systematic technique that turns FDEs into its differential parts in a steady period and is described as [25–27]

$$\Delta S = \frac{\Delta \wp^\delta}{\Gamma(1 + \delta)}, \tag{16}$$

where ΔS is the slighter scale and $\Delta \wp$ is the greater scale. The time fractional K-S model reacts discontinuously on a slighter scale, particularly at the highest point whereas it anticipates a plane solitary wave on the greater scale. Thus, Equation (11) is considered two-scale transform [28–30]. The outcomes of any study problem depend on the scale. For an observable scale, the fluid is consistent; therefore, Newton's laws can be applied; however, they are illegitimate at the molecular scale. If the motion is free of time, then Newton's law is acceptable; otherwise, it can be revoked.

4.1. Convergence Theorem. Let P and Q be the Banach spaces and $\varsigma : P \longrightarrow Q$ be a contraction nonlinear mapping. If the sequence generated by HPM such as

$$\eta_n(P, \wp) = \varsigma(\eta_{n-1}(P, \wp)) = \sum_{i=0}^{n-1} \eta_i(P, \wp), \quad n = 1,2,3, \cdots, \tag{17}$$

then the following conditions must be true:

(1) $\|\eta_n(P, \wp) - \eta(P, \wp)\| \leq \varphi^n \|\psi(P, \wp) - \eta(P, \wp)\|$

(2) $\eta_n(P, \wp)$ is always in the neighborhood of $\eta(P, \wp)$ meaning $\eta_n(P, \wp) \in B(\eta(P, \wp), r) = \{\eta^*(P, \wp)/\|\eta^*(P, \wp) - \eta(P, \wp)\|\}$

(3) $\lim_{n \longrightarrow \infty} \eta_n(P, \wp) = \eta(P, \wp)$

Proof.

(1) We prove condition (1) by induction on n, $\|\eta_1 - \eta\| = \|G(\eta_0) - \eta\|$, and according to the Banach fixed point theorem, ς has a fixed point η meaning $\varsigma(\eta) = \eta$; therefore,

$$\|\eta_1 - \eta\| = \|G(\eta_0) - \eta\| = \|G(\eta_0) - G(\eta)\| \leq \varphi \|\eta_0 - \eta\| = \varphi \|\psi(P, \wp) - \eta\|, \tag{18}$$

since ς is a contraction mapping. Assume that $\|\eta_{n-1} - \eta\| \leq \varphi^{n-1} \|\psi(P, 0) - \eta(P, \wp)\|$ is an induction hypothesis, then

$$\|\eta_n - \eta\| = \|G(\eta_{n-1}) - G(\eta)\| \leq \varphi \|\eta_{n-1} - \eta\| \leq \varphi \varphi^{n-1} \|\psi(P, \wp) - \eta\| \tag{19}$$

(2) The first concern is to demonstrate that $\psi(P, \wp) \in B(\eta(P, \wp), r)$, and this is achieved by induction on m. So, for $m = 1$, $\|\psi(P, \wp) - \eta(P, \wp)\| = \|\eta(P, 0) - \eta(P, \wp)\| \leq r$ with $\eta(P, 0)$ the initial condition. Assume that $\|\psi(P, \wp) - \eta(P, \wp)\| \leq r$ for $m - 2$ is an induction hypothesis, then

$$\begin{aligned} \|\psi(P, \wp) - \eta(P, \wp)\| &= \psi_{m-2}(P, \wp) - \frac{f_m(P)}{\Gamma(\delta - m + 1)} \wp^{\delta - m} \Big\| \\ &\leq \|\psi_{m-1}(P, \wp) - \eta(P, \wp)\| + \left\| \frac{f_m(P)}{\Gamma(\delta - m + 1)} \wp^{\delta - m} \right\| = r. \end{aligned} \tag{20}$$

Now, for all $n \geq 1$, using condition (1), we have

$$\|\eta_n - \eta\| \leq \varphi^n \|\psi(P,\wp) - \eta\| \leq \varphi^n r \leq r. \quad (21)$$

(3) Using condition (2) and the fact that $\lim_{n\longrightarrow\infty}\phi^n = 0$ yields that $\lim_{n\longrightarrow\infty}\|\eta_n - \eta\| = 0$; therefore,

$$\lim_{n\longrightarrow\infty} \eta_n = \eta. \quad (22)$$

Thus, η converges. □

5. Numerical Examples

In this segment, we implement a two-scale method to achieve the approximate solution of the K-S model in one dimension. Results disclose that this approach is an extremely efficient and powerful aid for solving FDEs.

5.1. Example 1. Consider the K-S model in one dimension given as

$$\begin{aligned} \frac{\partial^\delta \eta}{\partial \wp^\delta} &= a\frac{\partial^2 \eta}{\partial \mathfrak{J}^2} - \frac{\partial}{\partial \mathfrak{J}}\left(\eta \frac{\partial}{\partial \mathfrak{J}}\chi(\varsigma)\right), \\ \frac{\partial^\delta \varsigma}{\partial \wp^\delta} &= b\frac{\partial^2 \varsigma}{\partial \mathfrak{J}^2} + c\eta - d\varsigma, \end{aligned} \quad (23)$$

with the initial conditions

$$\begin{aligned} \eta(\mathfrak{J},0) &= me^{-\mathfrak{J}^2}, \\ \varsigma(\mathfrak{J},0) &= ne^{-\mathfrak{J}^2}. \end{aligned} \quad (24)$$

Considering that the sensitivity function $\chi(\varsigma) = 0$; thus, the chemotactic term is zero, i.e., $\partial/\partial\mathfrak{J}(\eta\,\partial/\partial\mathfrak{J}\chi(\varsigma)) = 0$ and using

$$S = \frac{\wp^\delta}{\Gamma(1+\delta)}. \quad (25)$$

Thus, the coupled K-S model of Equation (23) becomes

$$\begin{aligned} \frac{\partial \eta}{\partial S} &= \frac{\partial \eta}{\partial S}, \\ \frac{\partial \varsigma}{\partial S} &= b\frac{\partial^2 \varsigma}{\partial \mathfrak{J}^2} + c\eta - d\varsigma. \end{aligned} \quad (26)$$

We can use HPM with He's polynomials on the system of Equation (26), and we get

$$\frac{\partial \eta_1}{\partial S} = a\frac{\partial^2 \eta_0}{\partial \mathfrak{J}^2}, \quad \eta_1(\mathfrak{J},0), \quad (27)$$

$$\frac{\partial \varsigma_1}{\partial S} = b\frac{\partial^2 \varsigma_0}{\partial \mathfrak{J}^2} + c\eta_0 - d\varsigma_0, \quad \varsigma_1(\mathfrak{J},0), \quad (28)$$

$$\frac{\partial \eta_2}{\partial S} = a\frac{\partial^2 \eta_1}{\partial \mathfrak{J}^2}, \quad \eta_2(\mathfrak{J},0), \quad (29)$$

$$\frac{\partial \varsigma_2}{\partial S} = b\frac{\partial^2 \varsigma_1}{\partial \mathfrak{J}^2} + c\eta_1 - d\varsigma_1, \quad \varsigma_2(\mathfrak{J},0), \quad (30)$$

$$\frac{\partial \eta_3}{\partial S} = a\frac{\partial^2 \eta_2}{\partial \mathfrak{J}^2}, \quad \eta_3(\mathfrak{J},0), \quad (31)$$

$$\frac{\partial \varsigma_3}{\partial S} = b\frac{\partial^2 \varsigma_2}{\partial \mathfrak{J}^2} + c\eta_2 - d\varsigma_2, \quad \varsigma_3(\mathfrak{J},0). \quad (32)$$

With the help of Equation (24), we can get the following iterations:

$$\eta(\mathfrak{J},0) = me^{-\mathfrak{J}^2}, \quad (33)$$

$$\varsigma(\mathfrak{J},0) = ne^{-\mathfrak{J}^2}, \quad (34)$$

$$\eta_1(\mathfrak{J},S) = 2am\left[-1 + 2\mathfrak{J}^2\right]e^{-\mathfrak{J}^2}S, \quad (35)$$

$$\varsigma_1(\mathfrak{J},S) = \left[2bn\left(2\mathfrak{J}^2 - 1\right) + (cm - dn)\right]e^{-\mathfrak{J}^2}S, \quad (36)$$

$$\eta_2(\mathfrak{J},S) = 4a^2m\left[3 - 12\mathfrak{J}^2 + 4\mathfrak{J}^4\right]e^{-\mathfrak{J}^2}\frac{S^2}{2}, \quad (37)$$

$$\begin{aligned} \varsigma_2(\mathfrak{J},S) = \Big[&d(-cm + dn) + 2acm\left(-1 + 2\mathfrak{J}^2\right) \\ &+ 2b\left(-1 + 2\mathfrak{J}^2\right)(cm - 2dn) \\ &+ 4b^2\left(3 - 12\mathfrak{J}^2 + 4\mathfrak{J}^4\right)\Big]e^{-\mathfrak{J}^2}\frac{S^2}{2}, \end{aligned} \quad (38)$$

$$\eta_3(\mathfrak{J},S) = 8a^3m\left[-15 + 90\mathfrak{J}^2 - 60\mathfrak{J}^4 + 8\mathfrak{J}^6\right]e^{-\mathfrak{J}^2}\frac{S^3}{6}, \quad (39)$$

$$\begin{aligned} \varsigma_3(\mathfrak{J},S) = \Big[&d^2(cm - dn) + 2bd(-2cm + 3dn)\left(-1 + 2\mathfrak{J}^2\right) \\ &+ 4a^2cm\left(3 - 12\mathfrak{J}^2 + 4\mathfrak{J}^4\right) \\ &+ 4b^2(cm - 3dn)\left(3 - 12\mathfrak{J}^2 + 4\mathfrak{J}^4\right) \\ &+ 8b^3n\left(-15 + 90\mathfrak{J}^2 - 60\mathfrak{J}^4 + 8\mathfrak{J}^6\right) \\ &+ 2acm\left\{d - 2dx^2 + b\left(6 - 24\mathfrak{J}^2 + 8\mathfrak{J}^4\right)\right\}\Big]e^{-\mathfrak{J}^2}\frac{S^3}{6}. \end{aligned} \quad (40)$$

In the same way, other of the elements can be identified. So, the series solution of Equation (23) with the help of Equation (25) is as follows:

$$\begin{aligned} \eta(\mathfrak{J},\wp) = &me^{-\mathfrak{J}^2} + 2ame^{-\mathfrak{J}^2}\left[-1 + 2\mathfrak{J}^2\right]\left(\frac{\wp^\delta}{\Gamma(1+\delta)}\right) \\ &+ 2a^2me^{-\mathfrak{J}^2}\left[3 - 12\mathfrak{J}^2 + 4\mathfrak{J}^4\right]\left(\frac{\wp^\delta}{\Gamma(1+\delta)}\right)^2 \\ &+ \frac{4}{3}a^3me^{-\mathfrak{J}^2}\left[-15 + 90\mathfrak{J}^2 - 60\mathfrak{J}^4 + 8\mathfrak{J}^6\right]\left(\frac{\wp^\delta}{\Gamma(1+\delta)}\right)^3, \end{aligned} \quad (41)$$

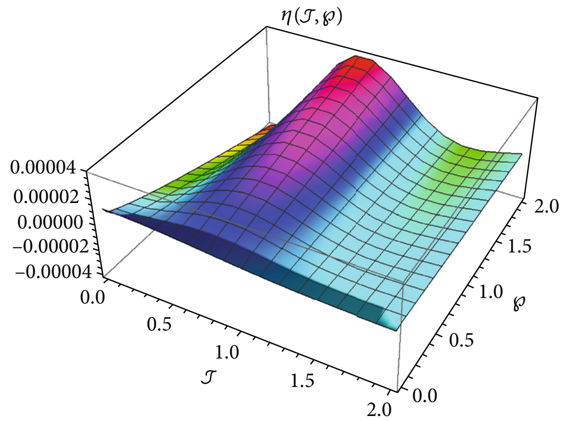

(a) Surface solution of $\eta(\mathfrak{I},\wp)$ when $\delta = 0.25$

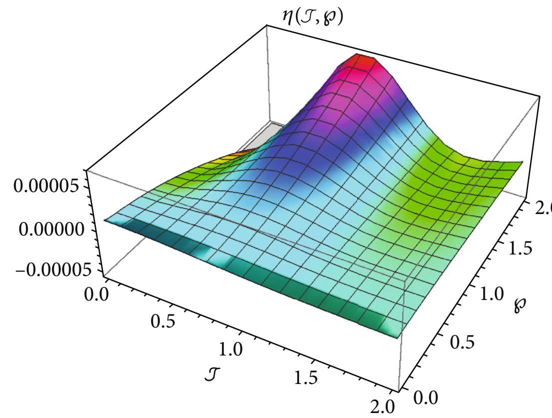

(b) Surface solution of $\eta(\mathfrak{I},\wp)$ when $\delta = 0.50$

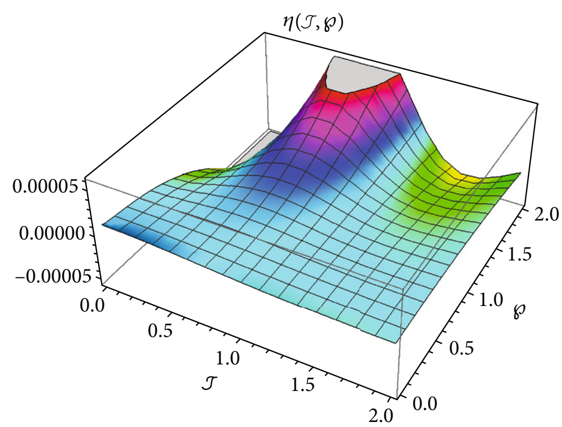

(c) Surface solution of $\eta(\mathfrak{I},\wp)$ when $\delta = 0.75$

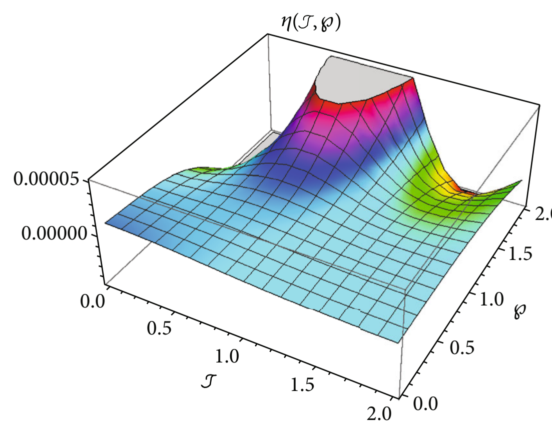

(d) Surface solution of $\eta(\mathfrak{I},\wp)$ when $\delta = 1$

Figure 1: The surface solution of $\eta(\mathfrak{I},\wp)$ for distinct values of δ.

$$\begin{aligned}
\varsigma(\mathfrak{I},\wp) = {} & n e^{-\mathfrak{I}^2} + \left[2bn\left(2\mathfrak{I}^2-1\right)+(cm-dn)\right]e^{-\mathfrak{I}^2}\left(\frac{\wp^{\delta}}{\Gamma(1+\delta)}\right) \\
& + \frac{1}{2}\left[d(-cm+dn)+2acm\left(-1+2\mathfrak{I}^2\right)\right. \\
& + 2b\left(-1+2\mathfrak{I}^2\right)(cm-2dn) \\
& \left. + 4b^2\left(3-12\mathfrak{I}^2+4\mathfrak{I}^4\right)\right]e^{-\mathfrak{I}^2}\left(\frac{\wp^{\delta}}{\Gamma(1+\delta)}\right)^2 \\
& + \frac{1}{6}\left[12b^2cm+4bcdm-120b^3n-36b^2dn\right. \\
& - 6bd^2n - d^3n - 48b^2cmx^2 - 8bcdmx^2 \\
& + 72b^3nx^2 144b^2dnx^2 + 12bd^2nx^2 + 16b^2cmx^4 \\
& - 48b^3nx^4 - 48b^2dnx^4 + 64b^3nx^6 + 4a^2cm\left(3-12\mathfrak{I}^2+4\mathfrak{I}^4\right) \\
& \left. + 2amc\left(d-2dx^2+b\left(6-24\mathfrak{I}^2+8\mathfrak{I}^4\right)\right)\right]e^{-\mathfrak{I}^2}\left(\frac{\wp^{\delta}}{\Gamma(1+\delta)}\right)^3.
\end{aligned} \tag{42}$$

Only some of terms are evaluated while the other terms can be obtained using the iterative formula. As a result, the solution of the system of Equation (23) is as follows:

$$\begin{aligned}
\eta(\mathfrak{I},\wp) &= \eta(\mathfrak{I},0)+\eta_1(\mathfrak{I},0)+\eta_2(\mathfrak{I},0)+\eta_3(\mathfrak{I},0)+\cdots, \\
\varsigma(\mathfrak{I},\wp) &= \varsigma(\mathfrak{I},0)+\varsigma_1(\mathfrak{I},0)+\varsigma_2(\mathfrak{I},0)+\varsigma_3(\mathfrak{I},0)+\cdots.
\end{aligned} \tag{43}$$

5.2. Example 2.

$$\begin{aligned}
\frac{\partial^{\delta}\eta}{\partial\wp^{\delta}} &= a\frac{\partial^2\eta}{\partial\mathfrak{I}^2} - \frac{\partial}{\partial\mathfrak{I}}\left(\eta\frac{\partial}{\partial\mathfrak{I}}\chi(\varsigma)\right), \\
\frac{\partial^{\delta}\varsigma}{\partial\wp^{\delta}} &= b\frac{\partial^2\varsigma}{\partial\mathfrak{I}^2} + c\eta - d\varsigma,
\end{aligned} \tag{44}$$

with the initial conditions

$$\begin{aligned}
\eta(\mathfrak{I},0) &= m e^{-\mathfrak{I}^2}, \\
\varsigma(\mathfrak{I},0) &= n e^{-\mathfrak{I}^2}.
\end{aligned} \tag{45}$$

Considering that the sensitivity function $\chi(\varsigma)=\varsigma$; thus, the chemotactic term becomes $\partial/\partial\mathfrak{I}(\eta\partial/\partial\mathfrak{I}\chi(h)) = \partial\eta/\partial\mathfrak{I}\, \partial h/\partial\mathfrak{I} + \eta\partial^2 h/\partial\mathfrak{I}^2$ and using

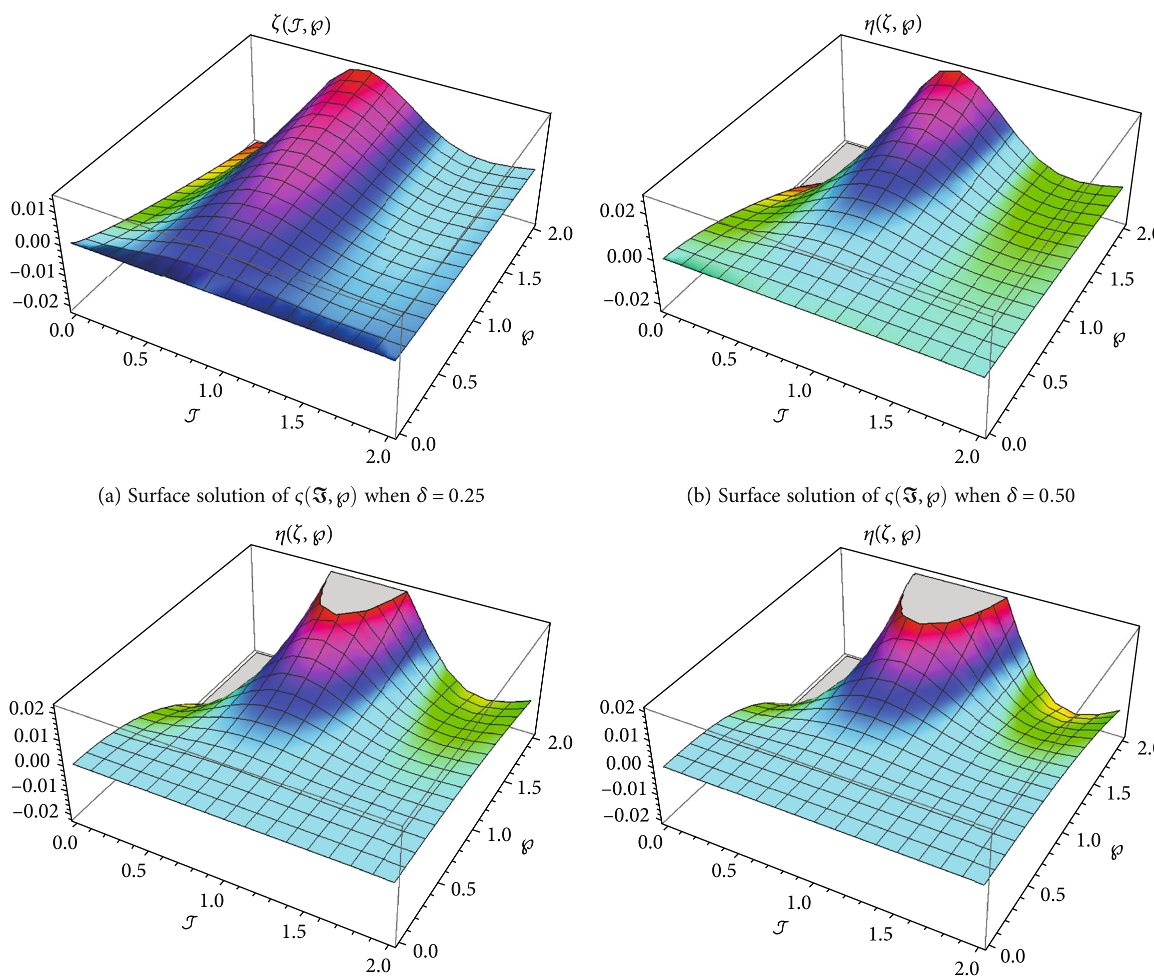

(a) Surface solution of $\varsigma(\mathfrak{I}, \wp)$ when $\delta = 0.25$

(b) Surface solution of $\varsigma(\mathfrak{I}, \wp)$ when $\delta = 0.50$

(c) Surface solution of $\varsigma(\mathfrak{I}, \wp)$ when $\delta = 0.75$

(d) Surface solution of $\varsigma(\mathfrak{I}, \wp)$ when $\delta = 1$

Figure 2: The surface solution of $\varsigma(\mathfrak{I}, \wp)$ for distinct values of δ.

$$S = \frac{\wp^{\delta}}{\Gamma(1+\delta)}. \tag{46}$$

Thus, the coupled K-S model of Equation (44) becomes

$$\frac{\partial \eta}{\partial S} = a\frac{\partial^2 \eta}{\partial \mathfrak{I}^2} - \frac{\partial \eta}{\partial \mathfrak{I}}\frac{\partial h}{\partial \mathfrak{I}} - \eta\frac{\partial^2 h}{\partial \mathfrak{I}^2}, \tag{47}$$

$$\frac{\partial \varsigma}{\partial S} = b\frac{\partial^2 \varsigma}{\partial \mathfrak{I}^2} + c\eta - d\varsigma. \tag{48}$$

Now, using the two-scale approach, with the help of Equation (45), we can get the following iterations directly

$$\eta(\mathfrak{I}, 0) = me^{-\mathfrak{I}^2}, \tag{49}$$

$$\varsigma(\mathfrak{I}, 0) = ne^{-\mathfrak{I}^2}, \tag{50}$$

$$\eta_1(\mathfrak{I}, S) = 2m\left[a\left(2\mathfrak{I}^2 - 1\right) - ne^{-\mathfrak{I}^2}\left(4\mathfrak{I}^2 - 1\right)\right]S, \tag{51}$$

$$\varsigma_1(\mathfrak{I}, S) = \left[2bn\left(2\mathfrak{I}^2 - 1\right) + (cm - dn)\right]e^{-\mathfrak{I}^2}S, \tag{52}$$

$$\begin{aligned}\eta_2(\mathfrak{I}, S) = 2me^{-3\mathfrak{I}^2}\Big[&-cme^{\mathfrak{I}^2}\left(-1 + 4\mathfrak{I}^2\right) \\ &+ 2a^2e^{2\mathfrak{I}^2}\left(3 - 12\mathfrak{I}^2 + 4\mathfrak{I}^4\right) \\ &- 2ane^{\mathfrak{I}^2}\left(7 - 58\mathfrak{I}^2 + 40\mathfrak{I}^4\right) \\ &+ n\Big\{de^{\mathfrak{I}^2}\left(-1 + 4\mathfrak{I}^2\right) - 2be^{\mathfrak{I}^2}\left(3 - 18\mathfrak{I}^2 + 8\mathfrak{I}^4\right) \\ &+ 2n\left(1 - 18\mathfrak{I}^2 + 24\mathfrak{I}^4\right)\Big\}\Big]\frac{S^2}{2},\end{aligned} \tag{53}$$

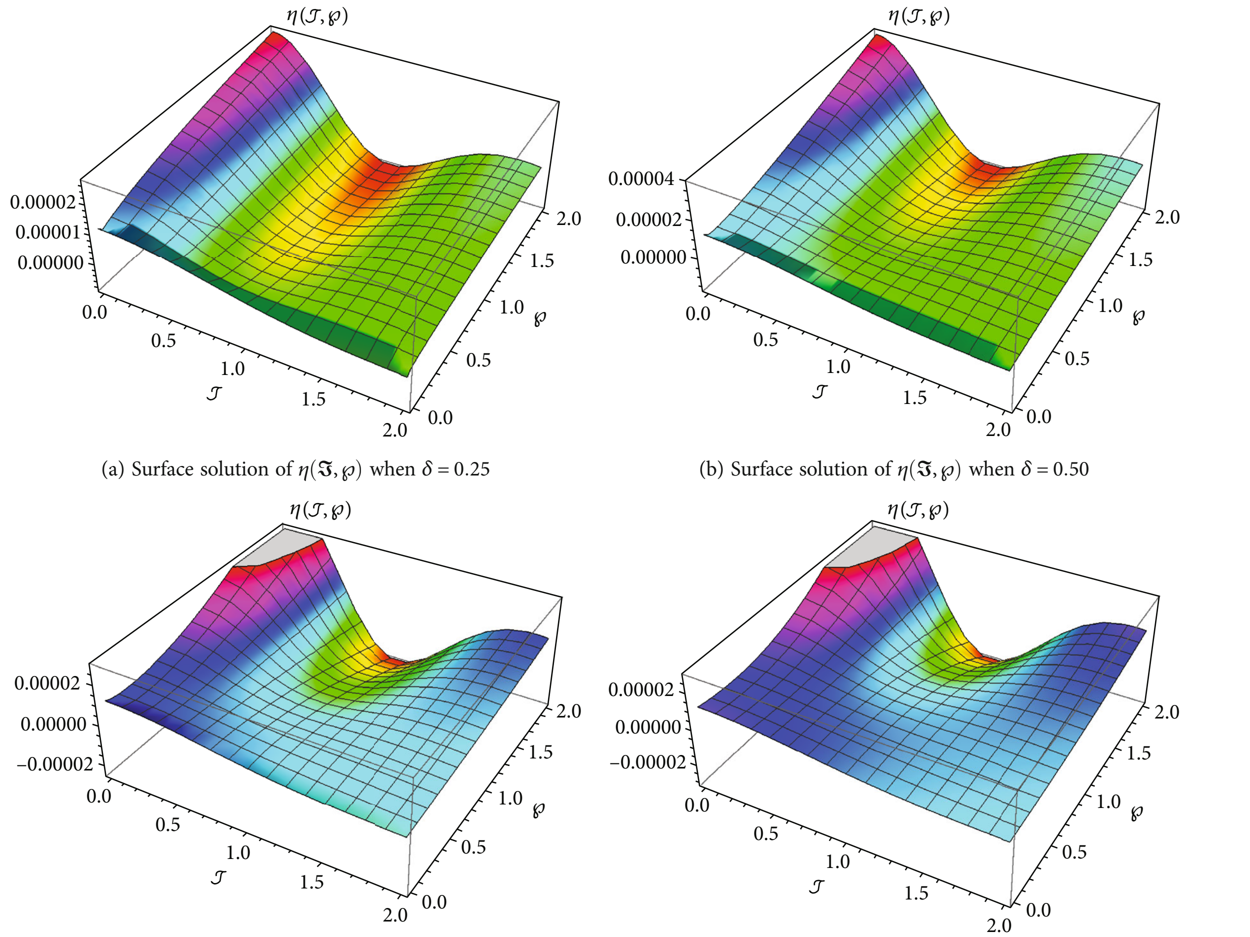

(a) Surface solution of $\eta(\mathfrak{T},\wp)$ when $\delta = 0.25$

(b) Surface solution of $\eta(\mathfrak{T},\wp)$ when $\delta = 0.50$

(c) Surface solution of $\eta(\mathfrak{T},\wp)$ when $\delta = 0.75$

(d) Surface solution of $\eta(\mathfrak{T},\wp)$ when $\delta = 1$

FIGURE 3: The surface solution of $\eta(\mathfrak{T},\wp)$ for distinct values of δ.

$$\begin{aligned}\varsigma_2(\mathfrak{T},S) = 2e^{-2\mathfrak{T}^2}\Big[&2b^2e^{\mathfrak{T}^2}n\left(3-12\mathfrak{T}^2+4\mathfrak{T}^4\right)\\ &+be^{\mathfrak{T}^2}\left(cm\left(-1+2\mathfrak{T}^2\right)+dn\left(1-6\mathfrak{T}-2\mathfrak{T}^2+4\mathfrak{T}^3\right)\right)\\ &+\mathfrak{T}\Big(-d^2e^{\mathfrak{T}^2}n-2ace^{\mathfrak{T}^2}m\left(-3+2\mathfrak{T}^2\right)\\ &+cm\left(de^{\mathfrak{T}^2}+4n\left(-3+4\mathfrak{T}^2\right)\right)\Big)\Big]\frac{S^2}{2}.\end{aligned} \tag{54}$$

In the same way, other of the elements can be identified. So, the series solution of Equation (44) with the help of Equation (46) is as follows:

$$\begin{aligned}\eta(\mathfrak{T},S) = &me^{-\mathfrak{T}^2}+2m\left[a\left(2\mathfrak{T}^2-1\right)-ne^{-\mathfrak{T}^2}\left(4\mathfrak{T}^2-1\right)\right]\left(\frac{\wp^\delta}{\Gamma(1+\delta)}\right)\\ &+me^{-3\mathfrak{T}^2}\Big[-cme^{\mathfrak{T}^2}\left(-1+4\mathfrak{T}^2\right)+2a^2e^{2\mathfrak{T}^2}\left(3-12\mathfrak{T}^2+4\mathfrak{T}^4\right)\\ &-2ane^{\mathfrak{T}^2}\left(7-58\mathfrak{T}^2+40\mathfrak{T}^4\right)+n\Big\{de^{\mathfrak{T}^2}\left(-1+4\mathfrak{T}^2\right)\\ &-2be^{\mathfrak{T}^2}\left(3-18\mathfrak{T}^2+8\mathfrak{T}^4\right)+2n\left(1-18\mathfrak{T}^2+24\mathfrak{T}^4\right)\Big\}\Big]\left(\frac{\wp^\delta}{\Gamma(1+\delta)}\right)^2,\end{aligned} \tag{55}$$

$$\begin{aligned}\varsigma(\mathfrak{T},S) = &ne^{-\mathfrak{T}^2}+e^{-\mathfrak{T}^2}\left[2bn\left(2\mathfrak{T}^2-1\right)+(cm-dn)\right]\left(\frac{\wp^\delta}{\Gamma(1+\delta)}\right)\\ &+e^{-2\mathfrak{T}^2}\Big[2b^2e^{\mathfrak{T}^2}n\left(3-12\mathfrak{T}^2+4\mathfrak{T}^4\right)+be^{\mathfrak{T}^2}\left(cm\left(-1+2\mathfrak{T}^2\right)\right.\\ &\left.+dn\left(1-6\mathfrak{T}-2\mathfrak{T}^2+4\mathfrak{T}^3\right)\right)+\mathfrak{T}\Big(-d^2e^{\mathfrak{T}^2}n-2ace^{\mathfrak{T}^2}m\left(-3+2\mathfrak{T}^2\right)\\ &+cm\left(de^{\mathfrak{T}^2}+4n\left(-3+4\mathfrak{T}^2\right)\right)\Big)\Big]\left(\frac{\wp^\delta}{\Gamma(1+\delta)}\right)^2.\end{aligned} \tag{56}$$

6. Results and Discussion

In this segment, we demonstrate the validity and the accuracy of the two-scale approach through the 3D graphical representations. We also present the graphical models and physical behaviors of the time-fractional K-S model. Mathematica program 11.0.1. is used to calculate the iterations and the graphical representations. Figures 1–4 show the surface graphs of the K-S model for $\eta(\mathfrak{T},\wp)$ and $\varsigma(\mathfrak{T},\wp)$, respectively, at different values of δ with $0 \le \mathfrak{T} \le 2$ and $0 \le \wp \le 2$. On behalf of graphical illustrations, we adopt $m = 0.000012$, $n = 0.000016$, $a = 0.5$, $b = 3$, $c = 1$, $d = 2$. The graphical illustrations have validated the convergence of fractional-order

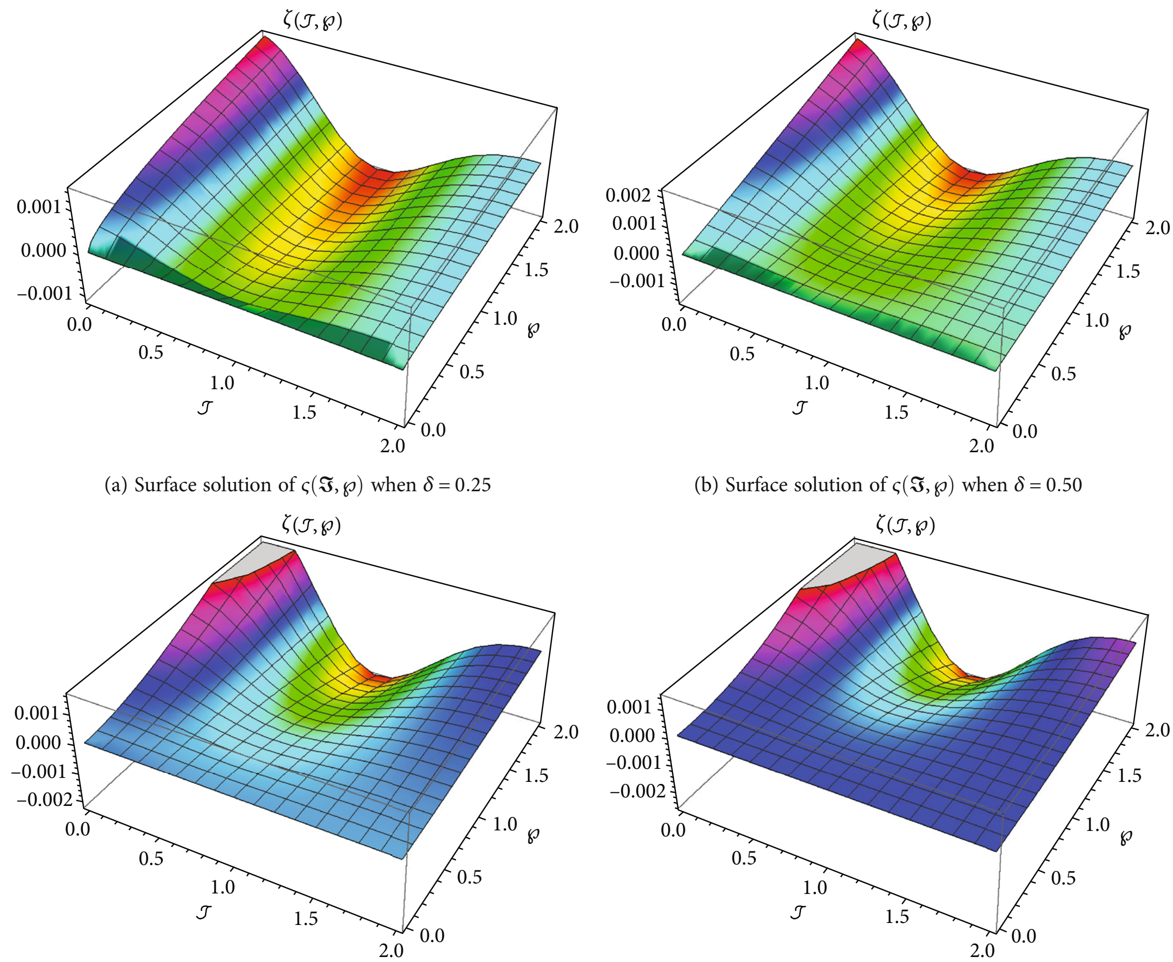

(a) Surface solution of $\varsigma(\mathfrak{T}, \wp)$ when $\delta = 0.25$

(b) Surface solution of $\varsigma(\mathfrak{T}, \wp)$ when $\delta = 0.50$

(c) Surface solution of $\varsigma(\mathfrak{T}, \wp)$ when $\delta = 0.75$

(d) Surface solution of $\varsigma(\mathfrak{T}, \wp)$ when $\delta = 1$

Figure 4: The surface solution of $\varsigma(\mathfrak{T}, \wp)$ for distinct values of δ.

solutions in the direction of integer-order solutions. We calculate the iteration only up to 3 terms, and the series of the solution converges to the exact solution very rapidly. Some more iterations can be evaluated for more accuracy of the approximate solutions. It is noted that the obtained solutions are similar which legitimize the reliability of the proposed strategies:

7. Conclusion

In this study, we have successfully applied a hybrid strategy where FCT has coupled with HPM to investigate the approximate solution of the nonlinear time fractional K-S model. The current association is not just helpful for fractional-order differential equations but also other differential equations with some variants. The main advantage of FCT is that it deals with the nonlinear problems straightforward to customize FDEs into their differential parts. We performed two numerical illustrations of the fractional K-S model to examine the reliability of the suggested approach. The results indicate that the two-scale approach is a more effective and powerful strategy in determining the analytical solutions of nonlinear differential equations. Thus, we conclude that our proposed scheme is suitable and can be considered for the other nonlinear fractional partial differential equations with fractal derivatives in future study.

Data Availability

All the data are available within the article.

Conflicts of Interest

The authors declare that they have no conflicts of interest.

Acknowledgments

This work was supported by the Foundation of Yibin University, China (Grant no. 2019QD07).

References

[1] D. Baleanu, J. A. T. Machado, and A. C. Luo, *Fractional dynamics and control*, Springer Science & Business Media, 2011.

[2] K. S. Miller and B. Ross, *An introduction to the fractional calculus and fractional differential equations*, Wiley, 1993.

[3] I. Podlubny, *Fractional differential equations: an introduction to fractional derivatives, fractional differential equations, to methods of their solution and some of their applications*, Elsevier, 1998.

[4] A. Atangana, "Numerical solution of space-time fractional derivative of groundwater flow equation," *Proceedings of the International Conference of Algebra and Applied Analysis*, vol. 2, p. 20, 2012.

[5] K. M. Owolabi, A. Atangana, and A. Akgul, "Modelling and analysis of fractal-fractional partial differential equations: application to reaction-diffusion model," *Alexandria Engineering Journal*, vol. 59, no. 4, pp. 2477–2490, 2020.

[6] G. W. Wang and T. Z. Xu, "The improved fractional sub-equation method and its applications to nonlinear fractional partial differential equations," *Romanian Reports in Physics*, vol. 66, no. 3, pp. 595–602, 2014.

[7] L. Debnath, "Recent applications of fractional calculus to science and engineering," *International Journal of Mathematics and Mathematical Sciences*, vol. 2003, 3442 pages, 2003.

[8] F. Haq, K. Shah, Q. M. Al-Mdallal, and F. Jarad, "Application of a hybrid method for systems of fractional order partial differential equations arising in the model of the one-dimensional Keller-Segel equation," *The European Physical Journal Plus*, vol. 134, no. 9, pp. 1–11, 2019.

[9] N. Bournaveas and V. Calvez, "The one-dimensional Keller–Segel model with fractional diffusion of cells," *Nonlinearity*, vol. 23, no. 4, pp. 923–935, 2010.

[10] I. R. Lapidus and R. Schiller, "A mathematical model for bacterial chemotaxis," *Biophysical Journal*, vol. 14, no. 11, pp. 825–834, 1974.

[11] H. Zhang, M. Nadeem, A. Rauf, and Z. G. Hui, "A novel approach for the analytical solution of nonlinear time-fractional di_erential equations," *International Journal of Numerical Methods for Heat & Fluid Flow*, vol. 31, no. 4, pp. 1069–1084, 2020.

[12] K.-L. Wang and S.-W. Yao, "He's fractional derivative for the evolution equation," *Thermal Science*, vol. 24, no. 4, pp. 2507–2513, 2020.

[13] J.-H. He and Z.-B. Li, "Converting fractional differential equations into partial differential equations," *Thermal Science*, vol. 16, no. 2, pp. 331–334, 2012.

[14] J.-H. He, "Homotopy perturbation technique," *Computer Methods in Applied Mechanics and Engineering*, vol. 178, no. 3-4, pp. 257–262, 1999.

[15] J. Biazar and H. Ghazvini, "Exact solutions for nonlinear Burgers' equation by homotopy perturbation method," *Numerical Methods for Partial Differential Equations*, vol. 25, no. 4, pp. 833–842, 2009.

[16] N. Anjum and J. H. He, "Homotopy perturbation method for N/MEMS oscillators," *Mathematical Methods in the Applied Sciences*, 2020.

[17] J. H. He and Y. O. El Dib, "Homotopy perturbation method for Fangzhu oscillator," *Journal of Mathematical Chemistry*, vol. 58, no. 10, pp. 2245–2253, 2020.

[18] H. M. Sedighi and F. Daneshmand, "Static and dynamic pull-in instability of multiwalled carbon nanotube probes by Hes iteration perturbation method," *Journal of Mechanical Science and Technology*, vol. 28, no. 9, pp. 3459–3469, 2014.

[19] V. F. Morales-Delgado, J. F. Gómez-Aguilar, S. Kumar, and M. A. Taneco-Hernández, "Analytical solutions of the Keller-Segel chemotaxis model involving fractional operators without singular kernel," *The European Physical Journal Plus*, vol. 133, no. 5, p. 200, 2018.

[20] A. Atangana, "Extension of the Sumudu homotopy perturbation method to an attractor for one- dimensional Keller-Segel equations," *Applied Mathematical Modelling*, vol. 39, no. 10-11, pp. 2909–2916, 2015.

[21] D. Sharma, G. S. Samra, and P. Singh, "Approximate solution for fractional attractor one-dimensional Keller-Segel equations using homotopy perturbation Sumudu transform method," *Nonlinear Engineering*, vol. 9, no. 1, pp. 370–381, 2020.

[22] H. Liu, H. Khan, R. Shah, A. A. Alderremy, S. Aly, and D. Baleanu, "On the fractional view analysis of Keller–Segel equations with sensitivity functions," *Complexity*, vol. 2020, 15 pages, 2020.

[23] S. Kumar, A. Kumar, and I. K. Argyros, "A new analysis for the Keller-Segel model of fractional order," *Numerical Algorithms*, vol. 75, no. 1, pp. 213–228, 2017.

[24] F. Li and M. Nadeem, "He–Laplace method for nonlinear vibration in shallow water waves," *Journal of Low Frequency Noise, Vibration and Active Control*, vol. 38, no. 3-4, pp. 1305–1313, 2019.

[25] R. W. Ibrahim, "Fractional complex transforms for fractional differential equations," *Advances in Difference Equations*, vol. 2012, no. 1, p. 192, 2012.

[26] J.-H. He, S. Elagan, and Z. Li, "Geometrical explanation of the fractional complex transform and derivative chain rule for fractional calculus," *Physics Letters A*, vol. 376, no. 4, pp. 257–259, 2012.

[27] Z.-B. Li and J.-H. He, "Fractional complex transform for fractional differential equations," *Mathematical and Computational Applications*, vol. 15, no. 5, pp. 970–973, 2010.

[28] Q. T. Ain and J.-H. He, "On two-scale dimension and its applications," *Thermal Science*, vol. 23, no. 3 Part B, pp. 1707–1712, 2019.

[29] J.-H. He, "Fractal calculus and its geometrical explanation," *Results in Physics*, vol. 10, pp. 272–276, 2018.

[30] Q. T. Ain, J.-H. He, N. Anjum, and M. Ali, "The fractional complex transform: a novel approach to the time-fractional Schrödinger equation," *Fractals*, vol. 28, no. 7, article 2050141, 2020.